The cornified envelope-bound ceramide fraction is altered in patients with atopic dermatitis

Boiten, W.A.; Smeden, J. van; Bouwstra, J.A.

CONFLICT OF INTEREST

AMT has received unrestricted grants from AbbVie and served on Advisory Boards for AbbVie. JMF has received honoraria from Novartis and served on their advisory board and has received research grant funding from AbbVie. BM and CG state no conflict of interest.

ACKNOWLEDGMENTS

We would like to thank all the patients and healthy volunteers for participating in this study.

AUTHOR CONTRIBUTIONS

Conceptualization: BM, AMT, JF; Data curation: CG; Formal analysis: BM; Funding Acquisition: JF; Investigation: BM; Resources: CG, AMT; Supervision: AMT, JF; Visualization: BM; Writing - original draft preparation: BM, JF; Writing - review and editing: BM, CG, AMT, and JF

Barry Moran[1], Catriona Gallagher[2], Anne Marie Tobin[2,3] and Jean M. Fletcher[1,3,*]

[1]School of Biochemistry and Immunology, Trinity College Dublin, Dublin, Ireland; [2]Department of Dermatology, Tallaght Hospital, Dublin, Ireland; and [3]School of Medicine, Trinity College Dublin, Dublin, Ireland

[*]Corresponding author e-mail: jean.fletcher@tcd.ie

REFERENCES

Basdeo SA, Moran B, Cluxton D, Canavan M, McCormick J, Connolly M, et al. Polyfunctional, pathogenic CD161+ Th17 lineage cells are resistant to regulatory T cell-mediated suppression in the context of autoimmunity. J Immunol 2015;195:528–40.

Boniface K, Bernard FX, Garcia M, Gurney AL, Lecron JC, Morel F. IL-22 inhibits epidermal differentiation and induces proinflammatory gene expression and migration of human keratinocytes. J Immunol 2005;174:3695–702.

Conrad C, Di Domizio J, Mylonas A, Belkhodja C, Demaria O, Navarini AA, et al. TNF blockade induces a dysregulated type I interferon response without autoimmunity in paradoxical psoriasis. Nat Commun 2018;9:25.

Friedrich M, Tillack C, Wollenberg A, Schauber J, Brand S. IL-36γ sustains a proinflammatory self-amplifying loop with IL-17C in anti-TNF-induced psoriasiform skin lesions of patients with Crohn's disease. Inflamm Bowel Dis 2014;20:1891–901.

Gregorio J, Meller S, Conrad C, Di Nardo A, Homey B, Lauerma A, et al. Plasmacytoid dendritic cells sense skin injury and promote wound healing through type I interferons. J Exp Med 2010;207:2921–30.

Grine L, Dejager L, Libert C, Vandenbroucke RE. An inflammatory triangle in psoriasis: TNF, type I IFNs and IL-17. Cytokine Growth Factor Rev 2015;26:25–33.

Guerra I, Pérez-Jeldres T, Iborra M, Algaba A, Monfort D, Calvet X, et al. Incidence, clinical characteristics, and management of psoriasis induced by anti-TNF therapy in patients with inflammatory bowel disease: A nationwide cohort study. Inflamm Bowel Dis 2016;22:894–901.

Kim J, Krueger JG. Highly effective new treatments for psoriasis target the IL-23/Type 17 T cell autoimmune axis. Annu Rev Med 2017;68:255–69.

Moran B, Sweeney CM, Hughes R, Malara A, Kirthi S, Tobin AM, et al. Hidradenitis suppurativa is characterized by dysregulation of the Th17:Treg cell axis, which is corrected by anti-TNF therapy. J Invest Dermatol 2017;137:2389–95.

Moy AP, Murali M, Kroshinsky D, Horn TD, Nazarian RM. T-helper immune phenotype may underlie 'paradoxical' tumour necrosis factor-alpha inhibitor therapy-related psoriasiform dermatitis. Clin Exp Dermatol 2018;43:19–26.

Mylonas A, Conrad C. Psoriasis: classical vs. paradoxical. The Yin-Yang of TNF and Type I interferon. Front Immunol 2018;9:2746.

Palucka AK, Blanck JP, Bennett L, Pascual V, Banchereau J. Cross-regulation of TNF and IFN-alpha in autoimmune diseases. Proc Natl Acad Sci USA 2005;102:3372–7.

Pfaff CM, Marquardt Y, Fietkau K, Baron JM, Lüscher B. The psoriasis-associated IL-17A induces and cooperates with IL-36 cytokines to control keratinocyte differentiation and function. Sci Rep 2017;7:15631.

Roederer M, Nozzi JL, Nason MC. SPICE: exploration and analysis of post-cytometric complex multivariate datasets. Cytometry A 2011;79:167–74.

Tillack C, Ehmann LM, Friedrich M, Laubender RP, Papay P, Vogelsang H, et al. Anti-TNF antibody-induced psoriasiform skin lesions in patients with inflammatory bowel disease are characterised by interferon-gamma-expressing Th1 cells and IL-17A/IL-22-expressing Th17 cells and respond to anti-IL-12/IL-23 antibody treatment. Gut 2014;63:567–77.

Toussirot É, Aubin F. Paradoxical reactions under TNF-alpha blocking agents and other biological agents given for chronic immune-mediated diseases: an analytical and comprehensive overview. RMD Open 2016;2:e000239.

Yu CF, Peng WM, Oldenburg J, Hoch J, Bieber T, Limmer A, et al. Human plasmacytoid dendritic cells support Th17 cell effector function in response to TLR7 ligation. J Immunol 2010;184:1159–67.

The Cornified Envelope-Bound Ceramide Fraction Is Altered in Patients with Atopic Dermatitis

Journal of Investigative Dermatology (2020) **140,** 1097–1100; doi:10.1016/j.jid.2019.09.013

TO THE EDITOR

The lipids covalently bound to the cornified envelope of corneocytes are essential for the human skin barrier (Swartzendruber et al., 1987). Together with the unbound lipids, they form a matrix regulating the permeability for water and pathogens through the stratum corneum (SC). Three main lipid classes are observed in the SC: sterols, fatty acids, and ceramides. Bound ceramides are a subset of the unbound ceramides and have an ultra-long omega-hydroxyl chain (OCer) (Farwanah et al., 2007; Hill et al., 2006). They are biosynthetically related to unbound linoleate esterified omega-hydroxyl ceramides (EOCers). Ceramide binding is selective, where ceramides with an unsaturated acyl chain (MuCers) and shorter chains are preferentially bound (Boiten et al., 2019). Yet, as both bound and unbound ceramides originate from the same precursors, compositional changes of precursors can affect both. Previously, changes in the unbound ceramide composition of patients with atopic dermatitis (AD) were observed. These changes correlated to decreased barrier function and altered lipid organization (Ishikawa et al., 2010; Janssens et al., 2012). Changes in bound ceramide composition were observed in autosomal recessive congenital ichthyosis and psoriasis and in atopic dogs

Abbreviations: AD, atopic dermatitis; EOCer, linoleate esterified omega-hydroxyl ceramide; MCL, mean carbon chain length; MuCer, ceramide with an unsaturated acyl chain; OCer, omega-hydroxyl ceramide; S-subclass, sphingosine subclass; SC, stratum corneum

Accepted manuscript published online 17 October 2019; corrected proof published online 19 December 2019

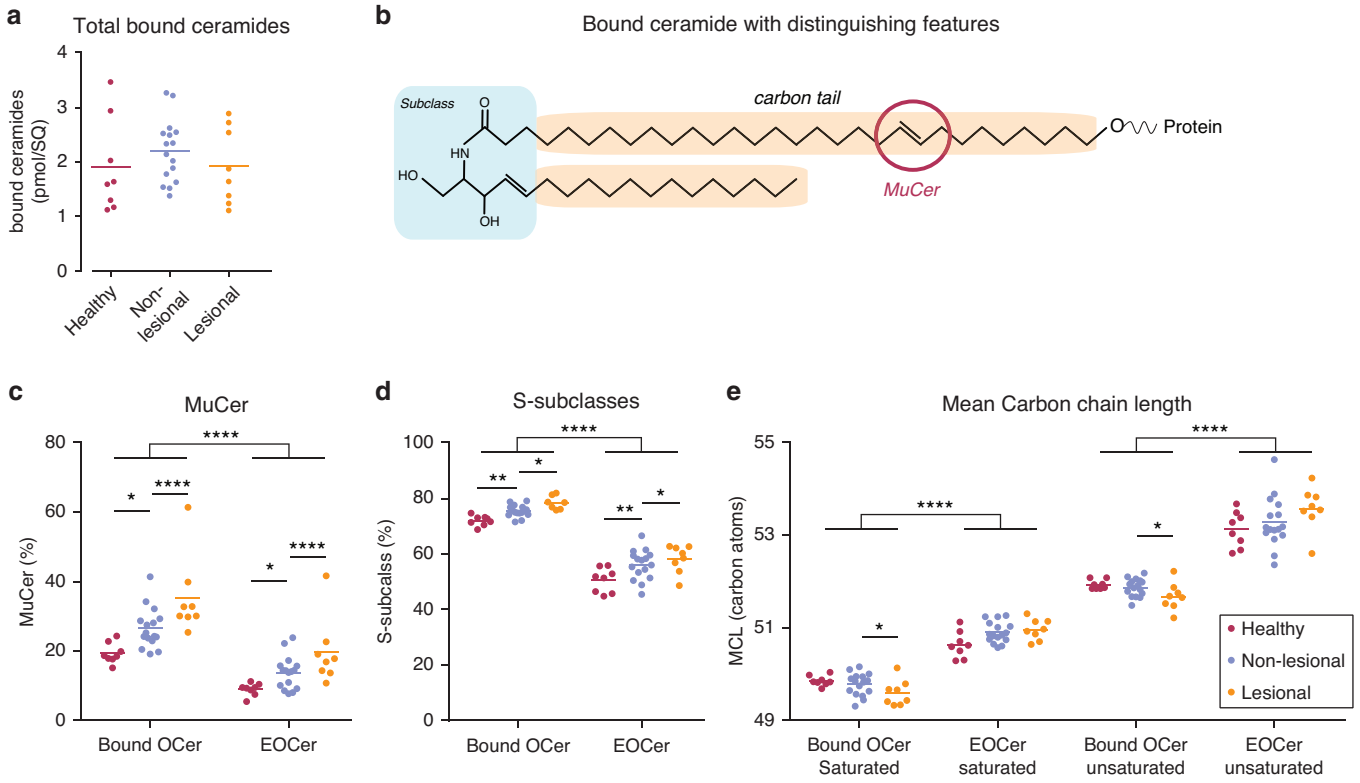

Figure 1. Atopic dermatitis–related changes in bound ceramide composition. (**a**) The amount of bound ceramide detected in pmol/SquameScan value in the tape-stripped samples of healthy, nonlesional, and lesional SC. (**b**) The structure of a bound OCer (OS C48:1) with three distinguishing features of the chemical structure indicated: the carbon tail length (orange), the hydrophilic head group defining the ceramide subclass (blue), and an unsaturated acyl chain (circled). (**c**) The percentage of unsaturation in the bound and unbound EOCers fractions. (**d**) The percentage of S-subclass ceramides in the bound and unbound EOCers fractions. (**e**) The MCL in the saturated and unsaturated bound ceramides and the MCL of the saturated and unsaturated EOCers. For the EOCers, 18 carbons were subtracted compensating for the linoleic acid. The MCL of the saturated and unsaturated ceramides are depicted separately. Significance indications are as follows: $*P \leq 0.05$, $**P \leq 0.01$, $***P \leq 0.005$, $****P \leq 0.001$. Significance of interactions is not indicated and can be found in Supplementary Table S3. EOCer, linoleate esterified omega-hydroxyl ceramide; MCL, mean carbon chain length; MuCer, ceramide with an unsaturated acyl chain; OCer, omega-hydroxyl ceramide; S-subclass, sphingosine subclass; SC, stratum corneum; SQ, SquameScan

and mice (Fujii et al., 2018; Grond et al., 2017; Popa et al., 2011; Wertz et al., 1989). It is hypothesized that the bound ceramide composition of patients with AD deviates and contributes to AD pathology. To our knowledge, no detailed liquid chromatography–mass spectrometry analysis of bound ceramides in patients with AD has been reported.

Here, we applied a quantitative liquid chromatography–mass spectrometry method to SC samples of patients with AD (Boiten et al., 2016). Samples were obtained after institutional approval and written informed consent, according to the Declaration of Helsinki. From eight healthy volunteers and 16 patients with AD, a 1.6-cm diameter nonlesional site on the ventral forearm was sequentially tape-stripped. A second tape-strip sample was obtained from lesional sites at the ventral forearm of eight patients with AD. Tapes were measured with a SquameScan (Heiland Electronic, Wetzlar, Germany) to determine the amount of SC stripped. Both bound and unbound lipids were extracted from tapes 9–12, as described elsewhere (Boiten et al., 2019). Before tape-stripping, transepidermal water loss was measured to determine the skin barrier function.

Liquid chromatography–mass spectrometry analysis did not show a decreased bound ceramide amount in AD, contrary to what others observed

Table 1. Correlation Coefficients and *P*-Values of Bound Ceramide Composition Compared with Barrier Function

	TEWL (g/cm²/h)	
Feature	**Pearson *r***	***P*-value**
MuCer (%)	0.731	<0.001
S-subclass (%)	0.692	<0.001
Difference MCL saturated (carbons)	0.561	0.001
Difference MCL MuCer (carbons)	0.231	0.203

Abbreviations: EOCer, linoleate esterified omega-hydroxyl ceramide; MCL, mean carbon chain length; MuCer, ceramide with an unsaturated acyl chain; OCer, omega-hydroxyl ceramide; S-subclass, sphingosine subclass; TEWL, transepidermal water loss

Four different distinguishing features were used to describe the bound ceramide composition: MuCer percentage, the percentage of S-subclass ceramides, and the difference in MCL between the unbound EOCers and bound OCers. The MCL differences of saturated and unsaturated ceramides were examined separately, because MuCers had a higher chain length and an increased MuCer percentage would increase the MCL.

using thin layer chromatography (Macheleidt et al., 2002). Figure 1a depicts the total detected bound ceramide amount corrected by SquameScan. To examine the bound ceramide composition in more detail, ceramides were grouped using three distinguishing features of their molecular structures (Figure 1b): MuCers percentage, sphingosine-subclass (S-subclass) percentage, and mean carbon chain length (MCL). Supplementary Text S1 explains the linear mixed modeling. The models compare patients with AD to healthy controls and a lesional site to the same patient's nonlesional site. Figure 1c and Supplementary Table S1 show that patients with AD had a 6.0% increase of bound MuCers, which further increased by 7.1% at their lesional sites. EOCers had similar increases in MuCers. In the unbound ceramides of patients with AD, increased percentages of S-subclass ceramides were observed (Ishikawa et al., 2010; Janssens et al., 2011). Figure 1d and Supplementary Table S2 depict that in AD the bound S-subclass ceramides were increased with 4.5% and an additional 2.1% in lesional skin. Again, these changes were similar in unbound EOCers.

Examining the chain length distribution, it was observed that at lesional sites, relatively more short chain ceramides were bound, thereby depleting short-chain EOCers. To compare MCLs of OCers and EOCers, 18 carbons were subtracted from the latter, compensating for the linoleic acid moiety. The MCLs of saturated and unsaturated ceramides differed significantly and were examined as separate parameters but were affected similarly by AD and at lesional skin (Figure 1e and Supplementary Table S3). At lesional sites, the MCL of bound ceramides significantly decreased; however, nonlesional sites showed no significant decrease. The changes in the MCL because of AD and lesional skin were inverse and significantly different between bound OCers and EOCers. Supplementary Figure S2 shows the saturated ceramide chain length distribution of bound OCers and EOCers. Although the overall amount of EOCers decreased, short-chain EOCers were further depleted. In AD, decreased amounts of EOCers are thought to play an role in decreasing barrier function (van Smeden et al., 2014).

It was examined if changes in the composition of bound ceramides coincided with changes in barrier function. The three distinguishing ceramide features were compared with transepidermal water loss. Table 1 shows the Pearson *r* and corresponding *P*-value (Supplementary Figure S2 graphically displays the correlations). The increased MuCer and S-subclass percentages correlated to reduced barrier function. Previously, it was demonstrated that unbound unsaturated lipids can contribute to a more disorganized lipid matrix, thereby decreasing barrier function (Mojumdar et al., 2014). Although bound ceramides already have an increased MuCer percentage compared with unbound ceramides, a further increased percentage of MuCers could have a destabilizing effect, increasing SC permeability. To examine the correlation with depletion because of shorter chain ceramide binding, the difference in MCL between the bound OCers and EOCers was calculated. Saturation was included as a separate parameter. The difference in saturated ceramide MCL between EOCers and OCers correlated to SC barrier function.

In summary, the bound ceramide composition of patients with AD contained more MuCers and S-subclass ceramides in lesional and nonlesional sites than healthy SC and at lesional sites, the chain length was reduced. These alterations in composition correlated to a decreased barrier function. Although individual alterations correlated, this does not imply a direct causality. It is feasible that all changes in the bound and unbound lipid composition of patients with AD combined would compromise the integrity of the lipid organization and thereby decrease SC barrier function. Nonetheless, it is thought that the bound lipids function as a scaffold for the unbound lipids. The altered state of the bound ceramide composition could impair this scaffold function. Both changes in the synthesis of precursor lipids and changes in the binding process could have influenced the bound ceramide composition in AD (Boiten et al., 2019). Treatment in dogs and mice has shown to increase bound ceramides (Fujii et al., 2018; Popa et al., 2011), making bound ceramides a possible target for barrier repair treatment of AD.

Data availability statement

Datasets related to this article can be found at: https://dx.doi.org/10.17632/n48kv8ssy9.1 hosted at Mendeley data (Boiten and Walter (2019), "EO and O ceramides, TEWL in atopic dermatitis stratum corneum").

ORCIDs

Walter Boiten: http://orcid.org/0000-0001-9060-6222
Jeroen van Smeden: http://orcid.org/0000-0002-2728-2832
Joke Bouwstra: http://orcid.org/0000-0002-7123-6868

CONFLICT OF INTEREST

The authors state no conflict of interest.

ACKNOWLEDGMENTS

This research was financially supported by the Dutch Fountdation TTW (grant no. 12400).

AUTHOR CONTRIBUTIONS

Conceptualization: WB, JB; Data Curation: WB; Formal Analysis: WB; Funding Acquisition: JB; Investigation: WB, JVS; Methodology: WB, JVS; Project Administration: JB, JVS; Resources: JB; Software: WB; Supervision: JB; Validation: WB; Visualization: WB; Writing - Original Draft Preparation: WB; Writing - Review and Editing: WB, JVS, JB

Walter Boiten[1], Jeroen van Smeden[1,2] and Joke Bouwstra[1,*]

[1]Biotherapeutics, Leiden Academic Centre for Drug Research, Leiden University, Leiden, The Netherlands; and [2]Centre for Human Drug Research, Leiden, The Netherlands
[*]Corresponding author e-mail: bouwstra@lacdr.leidenuniv.nl

SUPPLEMENTARY MATERIAL

Supplementary material is linked to the online version of the paper at www.jidonline.org, and at https://doi.org/10.1016/j.jid.2019.09.013.

REFERENCES

Boiten W, Absalah S, Vreeken R, Bouwstra J, van Smeden J. Quantitative analysis of ceramides using a novel lipidomics approach with three dimensional response modelling. Biochim Biophys Acta 2016;1861:1652–61.

Boiten W, Helder R, van Smeden J, Bouwstra J. Selectivity in cornified envelop binding of ceramides in human skin and the role of LXR inactivation on ceramide binding. Biochim Biophys Acta Mol Cell Biol Lipids 2019;1864:1206–13.

Farwanah H, Pierstorff B, Schmelzer CE, Raith K, Neubert RH, Kolter T, et al. Separation and mass spectrometric characterization of covalently bound skin ceramides using LC/APCI-MS and nano-ESI-MS/MS. J Chromatogr

B Analyt Technol Biomed Life Sci 2007;852:562–70.

Fujii M, Ohyanagi C, Kawaguchi N, Matsuda H, Miyamoto Y, Ohya S, et al. Eicosapentaenoic acid ethyl ester ameliorates atopic dermatitis-like symptoms in special diet-fed hairless mice, partly by restoring covalently bound ceramides in the stratum corneum. Exp Dermatol 2018;27:837–40.

Grond S, Eichmann TO, Dubrac S, Kolb D, Schmuth M, Fischer J, et al. PNPLA1 deficiency in mice and humans leads to a defect in the synthesis of omega-O-Acylceramides. J Invest Dermatol 2017;137:394–402.

Hill J, Paslin D, Wertz PW. A new covalently bound ceramide from human stratum corneum -omega-hydroxyacylphytosphingosine. Int J Cosmet Sci 2006;28:225–30.

Ishikawa J, Narita H, Kondo N, Hotta M, Takagi Y, Masukawa Y, et al. Changes in the ceramide profile of atopic dermatitis patients. J Invest Dermatol 2010;130:2511–4.

Janssens M, van Smeden J, Gooris GS, Bras W, Portale G, Caspers PJ, et al. Lamellar lipid organization and ceramide composition in the stratum corneum of patients with atopic eczema. J Invest Dermatol 2011;131:2136–8.

Janssens M, van Smeden J, Gooris GS, Bras W, Portale G, Caspers PJ, et al. Increase in short-chain ceramides correlates with an altered lipid organization and decreased barrier function in atopic eczema patients. J Lipid Res 2012;53:2755–66.

Macheleidt O, Kaiser HW, Sandhoff K. Deficiency of epidermal protein-bound omega-hydroxyceramides in atopic dermatitis. J Invest Dermatol 2002;119:166–73.

Mojumdar EH, Helder RW, Gooris GS, Bouwstra JA. Monounsaturated fatty acids reduce the barrier of stratum corneum lipid membranes by enhancing the formation of a hexagonal lateral packing. Langmuir 2014;30:6534–43.

Popa I, Remoue N, Hoang LT, Pin D, Gatto H, Haftek M, et al. Atopic dermatitis in dogs is associated with a high heterogeneity in the distribution of protein-bound lipids within the stratum corneum. Arch Dermatol Res 2011;303:433–40.

Swartzendruber DC, Wertz PW, Madison KC, Downing DT. Evidence that the corneocyte has a chemically bound lipid envelope. J Invest Dermatol 1987;88:709–13.

van Smeden J, Janssens M, Gooris GS, Bouwstra JA. The important role of stratum corneum lipids for the cutaneous barrier function. Biochim Biophys Acta 2014;1841:295–313.

Wertz PW, Madison KC, Downing DT. Covalently bound lipids of human stratum corneum. J Invest Dermatol 1989;92:109–11.

Alterations of Immune and Keratinization Gene Expression in Papulopustular Rosacea by Whole Transcriptome Analysis

Journal of Investigative Dermatology (2020) **140,** 1100–1103; doi:10.1016/j.jid.2019.09.021

TO THE EDITOR

Papulopustular rosacea (PPR) is a chronic, incurable disease with limited systemic treatment options (Holmes et al., 2018; van Zuuren and Fedorowicz, 2016). Expanding knowledge of the molecular underpinnings provides future directions for investigation to better combat PPR.

Previous gene expression studies of PPR interrogated specific genes using microarray or quantitative reverse transcriptase–PCR and compared PPR and normal skin taken from separate individuals (Buhl et al., 2015; Dajnoki et al., 2017). We performed an unbiased whole transcriptome search for differentially expressed genes (DEGs) in PPR and adjacent nonlesional skin from the same individual. This design maximized the capture of gene expression changes because of PPR and minimized differences because of individual and anatomical site variation.

The primary analysis compared PPR ($n = 6$) versus adjacent nonlesional skin samples ($n = 6$) from the same cosmetic subunits of the lower face in the same patients. A group of unrelated individuals without PPR ($n = 9$) (normal skin samples) was accrued as an additional control, with biopsies taken from the same cosmetic subunit as PPR participants. Supplementary Table S1 shows the characteristics of all 15 study participants. Supplementary Figure S1 shows principal component analyses of gene expression from PPR, nonlesional, and normal skin samples.

PPR lesions demonstrated 487 DEGs when compared with adjacent nonlesional skin ($P_{adjusted} < 0.05$, adjusted for false discovery rate), with 290 increased (Supplementary Table S2a) and 197 decreased (Supplementary Table S2b), with heat map shown in Figure 1. Example DEGs and transcript levels in PPR, nonlesional, and normal samples are displayed in Supplementary Figure S2. Directionality of changes were confirmed by quantitative reverse transcriptase–PCR (Figure 2) and immunohistochemistry (Supplementary Figure S3).

Compared with the aforementioned number of DEGs, more were found in comparing PPR to normal skin from unrelated individuals, 916 DEGs (649 increased [Supplementary Table S3a] and 267 decreased [Supplementary Table S3b]). As this higher number of DEGs likely is due to individual differences as well as PPR pathology, our analysis focused on the comparison between PPR lesions and adjacent nonlesional skin, which were from the same individuals.

Immune-related DEGs that demonstrated a >2-fold increase in PPR compared with adjacent nonlesional skin include: *IL4I1* ($P_{adjusted} = 3.0 \times 10^{-8}$) (Frampton and Blair, 2018), *IL4R* ($P_{adjusted} = 4.7 \times 10^{-5}$) (Frampton and Blair, 2018), *TNFAIP2* ($P_{adjusted} = 2.63 \times 10^{-5}$) (Sbidian et al., 2017), *IL1B* ($P_{adjusted} = 2.81 \times 10^{-6}$) (Mertens and Singh, 2009), and *IL6* ($P_{adjusted} = 6.7 \times 10^{-4}$) (Mease et al., 2017).

Four other DEGs elevated in PPR compared with adjacent nonlesional skin are worthy of mention, even though they were increased by 2-fold or less, as inhibitors against their pathways exist. These include *IL17RA* ($P_{adjusted} = 0.040$) (Sbidian et al., 2017) (the DEG *S100A7A*, downstream of *IL17*, was

Abbreviations: DEG, differentially expressed gene; GO, Gene Ontology; PPR, papulopustular rosacea

Accepted manuscript published online 6 November 2019; corrected proof published online 17 December 2019

SUPPLEMENTARY TEXT S1

Statistical analysis

Statistical analysis was performed using linear mixed modeling in SPSS, version 24 (IBM, Armonk, NY). Volunteers' and patients' numbers were set as random variable (1 to 24); this enabled a paired comparison of the nonlesional and lesional sites within a patient. In all models, atopic dermatitis (AD) was set as a fixed variable, being either 0 or 1, indicating if the skin was healthy or from a patient, respectively. Lesional was set as a fixed variable nested within AD: AD(lesional). Hereby, the model takes into account that changes because of lesions can only occur in patients. This gives a separate value that indicates if lesional sites were different from nonlesional. A fixed variable named EOCers was made; this indicates if there was a difference between the groups of bound omega-hydroxyl ceramides (OCers) and unbound linoleate esterified omega-hydroxyl ceramides (EOCers).

For the statistical analysis of the percentage of ceramides with an unsaturated acyl chain, a model was made including all specifications described previously. Interaction terms between the fixed variables EOCers and AD and EOCers and the nested lesional effect were tested. These interactions describe if a change in ceramides with an unsaturated acyl chain because of AD or lesions was different in the EOCers compared with the OCers. Supplementary Figure S1 gives a schematic overview of this model. After running the model, the interactions had nonsignificant contributions. This showed that changes in ceramides with an unsaturated acyl chain because of AD and lesions were similar in bound OCers and EOCers. The interactions were excluded for the final model. The parameter estimates obtained with the model are shown in Supplementary Table S1. The intercept represents the healthy bound OCer group.

The same model that was used for the percentage of ceramides with an unsaturated acyl chain was used for the percentage of sphingosine subclass ceramides. Again, a nonsignificant contribution of interaction was observed, indicating that the changes in sphingosine subclass percentage did not differ for bound OCers and EOCers. The parameter estimates observed after excluding the interactions are shown in Supplementary Table S2.

To examine the mean carbon chain length (MCL), a fixed factor for saturation was added to the model. This indicated if there was a difference in MCL between the saturated and unsaturated ceramides. This gives an additional interaction and another level of three-way interactions. The interaction between AD and lesional skin and saturation was added and the interaction between saturation and EOCers was added. The three-way interactions between AD and lesional skin with EOCer and saturation were added. This describes if the change in MCL because of AD or lesions in either the bound OCers or EOCers was different because of saturation. By running the model, it was shown that the three-way interactions were not significant and they were excluded. The interactions of saturation with AD and lesional skin were nonsignificant and were excluded as well. Supplementary Table S3 depicts the results of the final model. The interactions between the EOCers and AD and EOCers and lesions were significant. This showed that the change in MCL because of AD and lesions was different in the bound OCers compared with the unbound EOCers. Furthermore, the interaction between EOCers and saturation was significant. This showed that the change in MCL between OCers and EOCers was different between saturated and unsaturated ceramides.

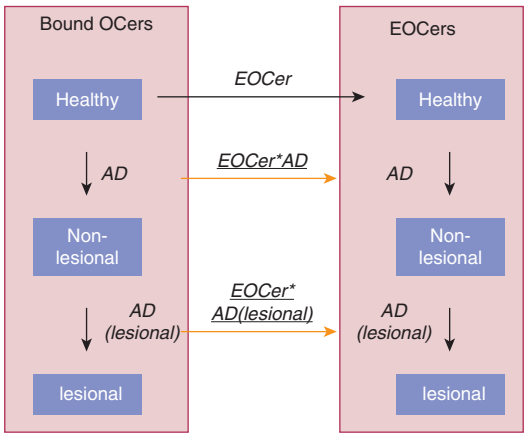

Supplementary Figure S1. Schematic representation of the LMM. Groups are indicated in blue boxes, fixed effects are indicated by italics, and interactions are underlined and in italics. AD, atopic dermatitis; EOCer, linoleate esterified omega-hydroxyl ceramide; LMM, linear mixed model; OCer, omega-hydroxyl ceramide.

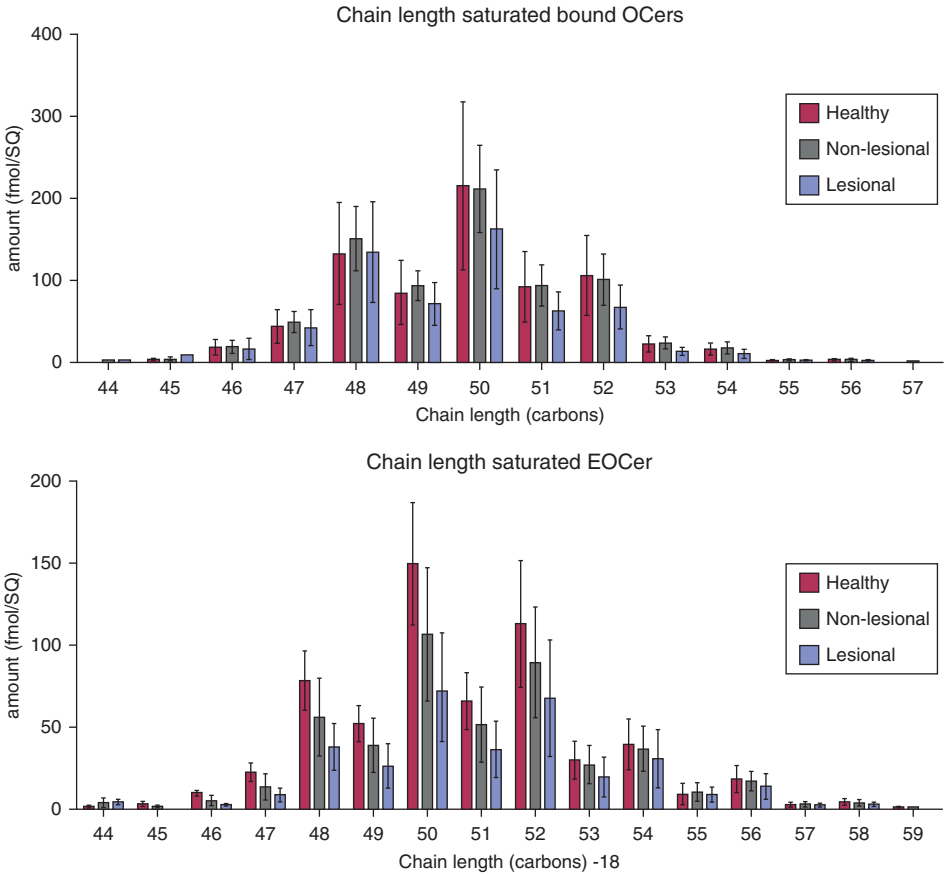

Supplementary Figure S2. Comparing the chain length distribution. The carbon chain length distribution of the bound OCers and unbound EOCers is depicted. For the EOCers, 18 carbons were subtracted to compensate for the linoleic acid. The amount is given in fmol per amount of stripped SC measured as SquameScan. The data is depicted as mean ± SD (healthy n = 8, nonlesional n = 16, lesional n = 8). EOCer, linoleate esterified omega-hydroxyl ceramide; OCer, omega-hydroxyl ceramide; SC, stratum corneum; SD, standard deviation; SQ, SquameScan.

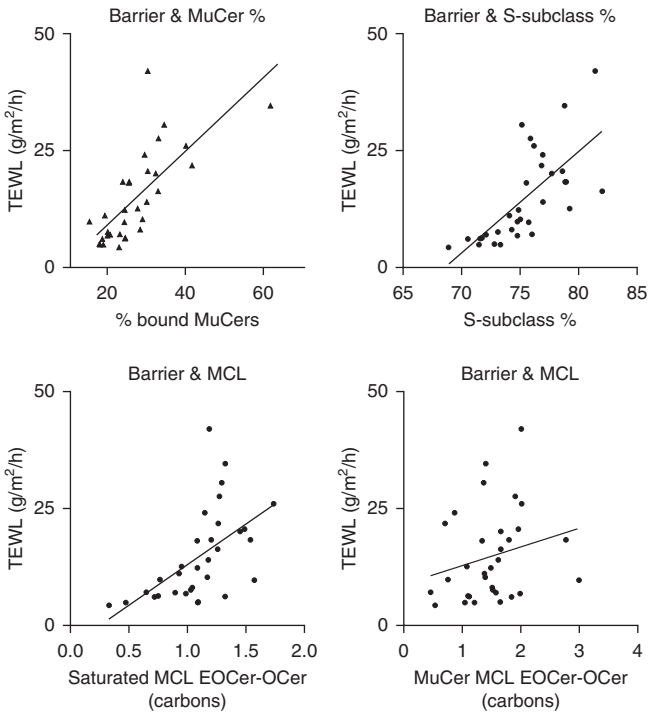

Supplementary Figure S3. Graphical depiction of correlations with barrier function. Each graph shows the TEWL compared with a different parameter. The line depicts a linear regression between the points indicating the correlation coefficient. EOCer, linoleate esterified omega-hydroxyl ceramide; MCL, mean carbon chain length; MuCer, ceramide with an unsaturated acyl chain; OCer, omega-hydroxyl ceramide; S-subclass, sphingosine subclass; TEWL, transepidermal water loss.

Supplementary Table S1. Linear Mixed Model Output for MuCer %

			95% confidence interval	
MuCer %	**Estimate**	***P*-value**	**Lower**	**Upper**
Intercept (Healthy bound)	20.58	<0.001	16.54	24.62
EOCer	−12.96	<0.001	−15.29	−10.62
AD	6.03	0.015	1.27	10.80
AD(Lesional)	7.07	<0.0001	3.94	10.20

Abbreviations: AD, atopic dermatitis; EOCer, linoleate esterified omega-hydroxyl ceramide; MuCer, ceramide with an unsaturated acyl chain.

The table shows the output for the fixed variables of the linear mixed model. The estimate of the intercept and effect sizes is given. The *P*-value and 95% intervals are given to interpret the output.

Supplementary Table S2. Output of the LMM Used to Compare the Percentage of S-Subclasses

			95% confidence interval	
S-Subclass %	**Estimate**	***P*-value**	**Lower**	**Upper**
Intercept (Healthy bound)	71.43	<0.001	69.02	73.84
EOCer	−20.18	<0.001	−21.66	−18.70
AD	4.50	0.003	1.67	7.32
AD(Lesional)	2.64	0.010	0.67	4.61

Abbreviations: AD, atopic dermatitis; EOCer, linoleate esterified omega-hydroxyl ceramide; LMM, linear mixed model; S-subclass, sphingosine subclass.

The table shows the output for the fixed variables of the linear mixed model. The estimate of the intercept and effect sizes is given. The *P*-value and 95% intervals are given to interpret the output.

Supplementary Table S3. Output of the LMM for the MCL Data

			95% confidence interval	
MCL	**Estimate**	***P*-value**	**Lower**	**Upper**
Intercept	49.84	<0.001	49.66	50.03
AD	−0.07	0.511	−0.28	0.14
AD(Lesional)	−0.23	0.008	−0.40	−0.06
EOCer	0.80	<0.001	0.59	1.01
Saturation	2.09	<0.001	1.97	2.22
Interactions				
AD*EOCer	0.28	0.016	0.05	0.51
AD(Lesional)*EOCer	0.37	0.002	0.15	0.60
Saturation* EOCer	0.38	<0.001	0.20	0.57

Abbreviations: AD, atopic dermatitis; EOCer, linoleate esterified omega-hydroxyl ceramide; LMM, linear mixed model; MCL, mean carbon chain length.

The table shows the output for the fixed variables of the linear mixed model. The estimate of the intercept and effect sizes is given. The *P*-value and 95% intervals are given to interpret the output.